

# Quantum Adaptive Self-Attention for Quantum Transformer Models

Chi-Sheng Chen<sup>1</sup> and En-Jui Kuo<sup>2</sup>

<sup>1</sup>Neuro Industry Research, Neuro Industry, Inc., Boston, MA, USA

<sup>2</sup>Department of Electrophysics, National Yang Ming Chiao Tung University, Hsinchu, Taiwan, R.O.C.

Transformer models have revolutionized sequential learning across various domains, yet their self-attention mechanism incurs quadratic computational cost, posing limitations for real-time and resource-constrained tasks. To address this, we propose Quantum Adaptive Self-Attention (QASA), a novel hybrid architecture that enhances classical Transformer models with a quantum attention mechanism. QASA replaces dot-product attention with a parameterized quantum circuit (PQC) that adaptively captures inter-token relationships in the quantum Hilbert space. Additionally, a residual quantum projection module is introduced before the feedforward network to further refine temporal features. Our design retains classical efficiency in earlier layers while injecting quantum expressiveness in the final encoder block, ensuring compatibility with current NISQ hardware. Experiments on synthetic time-series tasks demonstrate that QASA achieves faster convergence and superior generalization compared to both standard Transformers and reduced classical variants. Preliminary complexity analysis suggests potential quantum advantages in gradient computation, opening new avenues for efficient quantum deep learning models.

## 1 Introduction

Transformer architectures [VSP<sup>+</sup>17] have emerged as the backbone of modern deep learning, powering state-of-the-art models in natural language processing, vision, and sequential prediction. Their core strength lies in the self-attention mechanism, which models long-range dependencies dynamically. However, this comes at a significant computational cost—quadratic in sequence length—hindering real-time applications and large-scale deployment.

Meanwhile, quantum computing has introduced new paradigms in learning representations through entanglement and high-dimensional Hilbert spaces. Motivated by this, we explore the fusion of quantum computing and Transformers, focusing on enhancing attention mechanisms with quantum adaptability.

In this work, we introduce Quantum Adaptive Self-Attention (QASA)—a hybrid classical-quantum attention module designed to replace traditional dot-product operations with a learnable parameterized quantum circuit. Unlike purely quantum or classical models, QASA offers a practical balance: classical encoder layers ensure stable training, while a quantum-enhanced final layer boosts expressiveness and captures non-classical correlations.

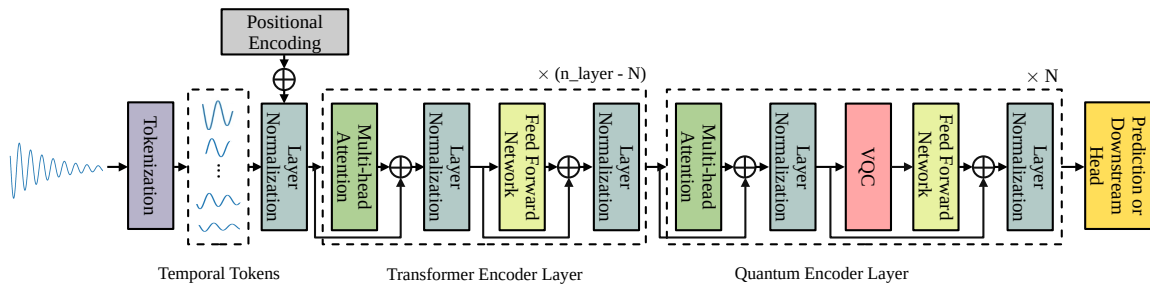


Figure 1: QASA model Architecture.

## 1.1 Our contributions

- **Quantum Adaptive Self-Attention Transformer Block (QASA):** We propose a quantum residual attention mechanism integrated into a Transformer architecture.
- **Quantum Feature Enhancement Layer:** We introduce a quantum projection layer that refines sequence features prior to final prediction.
- We empirically demonstrate the effectiveness of QASA in time-series forecasting, supported by theoretical insights on quantum complexity benefits.

## 2 Related work

### 2.1 Deep Learning on Time-Series Data

Deep learning has significantly advanced the modeling and understanding of time-series data across various domains. Recurrent Neural Networks (RNNs) [SP97], particularly Long Short-Term Memory (LSTM) networks [HS97] and Gated Recurrent Units (GRUs) [CGCB14], have been widely adopted due to their ability to capture long-term temporal dependencies. However, their sequential nature limits parallelization and increases training time. To address this, temporal convolutional networks (TCNs) [LFV<sup>+</sup>17] and Transformer-based architectures [VSP<sup>+</sup>17] have demonstrated superior performance by enabling parallel processing and better long-range dependency modeling.

Recent work in biomedical domains, such as electroencephalography (EEG), has utilized deep learning models to capture non-linear temporal dynamics in brain activity. Convolutional neural network-Transformer hybrids and attention-based models have shown success in tasks like motor imagery classification [CW24a], seizure detection [CCT25b], response prediction [LCC<sup>+</sup>23] and visual stimuli estimation [CW24b, Che24]. In industrial applications, particularly supply chain demand forecasting, Transformer variants such as the Temporal Fusion Transformer (TFT) [LALP21] and Informer [ZZP<sup>+</sup>21] have been applied to multi-horizon prediction tasks with irregular time intervals and exogenous variables. Similar time series learning techniques have been applied successfully in Molecule dynamics and even open quantum systems [TFX<sup>+</sup>22, TKT20].

Despite these advancements, challenges remain in modeling noisy, sparse, or irregularly-sampled sequences—especially in domains like healthcare and logistics—motivating [CC25] the development of hybrid models that integrate domain-specific priors with general-purpose deep learning architectures.

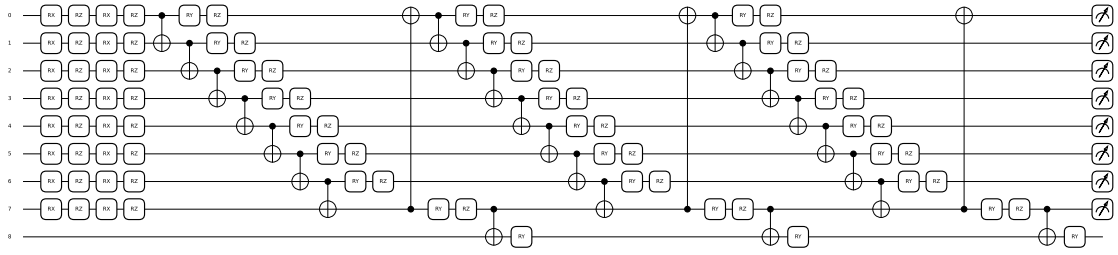


Figure 2: The variational quantum circuit (quantum neural network) used in this work.

## 2.2 Quantum Deep Learning on Time-Series Data

While classical deep learning has achieved remarkable success in time-series analysis, it often requires extensive computational resources and large-scale data to generalize effectively. With the advent of quantum computing, Quantum Deep Learning (QDL) [BWP<sup>+</sup>17] has emerged as a promising paradigm for modeling complex temporal patterns, offering theoretical advantages in expressivity and optimization through quantum entanglement and superposition.

In the context of time-series data, several quantum-inspired architectures have been proposed. Variational Quantum Circuits (VQCs) [GJ24] and Quantum Recurrent Neural Networks (QRNNs) [TMN<sup>+</sup>21] have been introduced to capture temporal dependencies using parameterized quantum gates and recurrent structures. A particularly notable development is the Quantum Long Short-Term Memory (QLSTM) network [CYF22], which integrates quantum circuits into the gating mechanisms of classical LSTMs. By replacing linear transformations with quantum operations, QLSTM models can potentially enhance memory capacity and temporal sensitivity, even in low-data regimes.

Applications of these models span multiple domains. In EEG signal analysis, hybrid QNN and quantum convolutional models have demonstrated improved efficiency in capturing spatiotemporal brainwave dynamics for tasks like motor imagery classification [CCTW24, CCT25a] and cognitive state detection [CTH24]. In finance and supply chain forecasting, quantum-enhanced LSTM architectures have been investigated for demand prediction and volatility modeling, leveraging quantum parallelism for more efficient scenario sampling and non-linear dynamics modeling [PS22].

Despite these advancements, research on Quantum Transformers for time-series data remains limited. Most existing studies focus on Quantum Visual Transformers (QViT) [CKM<sup>+</sup>22, KMCC24] in image-based tasks, leaving a gap in understanding how quantum self-attention mechanisms can be leveraged for sequential data. Addressing this gap is the key focus of this work. By exploring quantum self-attention architectures tailored to temporal patterns, we aim to provide novel insights and practical tools for efficient and expressive time-series modeling in quantum machine learning.

## 3 Methodology

### 3.1 Overview

We propose a hybrid quantum-classical Transformer model tailored for sequential data forecasting. The architecture is designed to capture temporal dependencies through classical attention mechanisms, while integrating a parameterized quantum circuit (PQC) to enhance the model’s expressiveness and representation power.

Layer	Operation	Input Shape	Output Shape
Input	Raw sequence	$(L, 1)$	$(L, 1)$
Linear Embedding	Linear + LayerNorm	$(L, 1)$	$(L, d)$
Positional Encoding	Add sinusoidal PE	$(L, d)$	$(L, d)$
Transformer Layer $\times(N-1)$	Multihead Attn + FFN	$(L, d)$	$(L, d)$
Quantum Encoder Layer	Self-Attn + QNN + FFN	$(L, d)$	$(L, d)$
QuantumLayer (QNN)	Linear $\rightarrow \mathbb{R}^n$		
	PQC $\rightarrow \mathbb{R}^n$	$(L, d)$	$(L, d)$
	Linear $\rightarrow \mathbb{R}^d$ + Residual		
Final Linear	Extract $h[L]$ and project	$(d)$	$(1)$

Table 1: Quantum Adaptive Self-Attention (QASA) Transformer Architecture. Each row lists a layer with its operation and input/output tensor shapes.  $L$  denotes the input sequence length (e.g.,  $L=50$ ),  $d$  is the hidden feature dimension (e.g.,  $d=256$ ), and  $n$  is the number of qubits in the quantum circuit (e.g.,  $n=8$ ). ‘Attn’ is an abbreviation for ‘attention’.

Given an input sequence  $x \in \mathbb{R}^{L \times 1}$  of length  $L$ , our model predicts a scalar target  $\hat{y} \in \mathbb{R}$  corresponding to the next value in the sequence.

### 3.2 Embedding and Positional Encoding

The input sequence is first projected into a high-dimensional space using a linear layer, followed by layer normalization:

$$h_0 = \text{LayerNorm}(W_e x + b_e), \quad h_0 \in \mathbb{R}^{L \times d}, \quad (1)$$

where  $d$  is the hidden dimension. We then apply fixed sinusoidal positional encoding to inject temporal order information:

$$h_0 \leftarrow h_0 + PE, \quad (2)$$

where  $PE$  denotes the positional encoding matrix.

### 3.3 Transformer Encoder Layers

The encoder consists of  $N$  layers, where the first  $N - 1$  layers are standard Transformer encoder layers defined as:

$$h_i = \text{Transformer}(h_{i-1}), \quad i = 1, \dots, N - 1. \quad (3)$$

The Transformer layer consists of two main sublayers: a multi-head self-attention mechanism and a position-wise feed-forward network (FFN). Each sublayer is wrapped with a residual connection and layer normalization. Formally, the computation of the  $i$ -th Transformer layer can be described as follows:

$$z_i = \text{LayerNorm}(h_{i-1} + \text{MultiHeadSelfAttention}(h_{i-1})), \quad (4)$$

$$h_i = \text{LayerNorm}(z_i + \text{FFN}(z_i)). \quad (5)$$

The multi-head self-attention mechanism is defined as:

$$\text{MultiHeadSelfAttention}(X) = \text{Concat}(\text{head}_1, \dots, \text{head}_H)W^O, \quad (6)$$

where each attention head is computed as:

$$head_j = \text{Attention}(XW_j^Q, XW_j^K, XW_j^V), \quad j = 1, \dots, H. \quad (7)$$

In the self-attention mechanism, each input vector is linearly projected into three different spaces to form the **query** ( $Q$ ), **key** ( $K$ ), and **value** ( $V$ ) matrices:

$$Q = XW^Q, \quad K = XW^K, \quad V = XW^V, \quad (8)$$

where  $X \in \mathbb{R}^{T \times d_{\text{model}}}$  is the input sequence (with  $T$  tokens), and  $W^Q, W^K, W^V \in \mathbb{R}^{d_{\text{model}} \times d_k}$  are learnable projection matrices.

The roles of  $Q$ ,  $K$ , and  $V$  are as follows:

- **Query** ( $Q$ ): Represents the current token's request for information.
- **Key** ( $K$ ): Represents the "content" or identity of each token in the sequence.
- **Value** ( $V$ ): Represents the actual information to be retrieved.

The attention mechanism computes a similarity score between each query and all keys:

$$\text{Attention}(Q, K, V) = \text{softmax} \left( \frac{QK^\top}{\sqrt{d_k}} \right) V. \quad (9)$$

This allows the model to retrieve contextually relevant information by weighting each value according to the query-key similarity.

The feed-forward network (FFN) is applied to each position separately and identically:

$$\text{FFN}(x) = \max(0, xW_1 + b_1)W_2 + b_2, \quad (10)$$

where  $W_1, W_2, b_1, b_2$  are learnable parameters.

Thus, the Transformer block can be summarized as:

$$z_i = \text{LayerNorm}(h_{i-1} + \text{MultiHeadSelfAttention}(h_{i-1})), \quad (11)$$

$$h_i = \text{LayerNorm}(z_i + \text{FFN}(z_i)), \quad (12)$$

$$\text{Transformer}(h_{i-1}) = h_i. \quad (13)$$

Each Transformer encoder layer includes multi-head self-attention, residual connections, and feedforward networks with GELU activation.

### 3.4 Quantum Encoder Layer

The final encoder block is a quantum-enhanced encoder layer. It begins with a multi-head self-attention module:

$$a = \text{MultiHeadAttention}(h_{N-1}) = \text{Concat}(head_1, \dots, head_h)W^O, \quad (14)$$

$$\text{where } head_i = \text{Attention}(QW_i^Q, KW_i^K, VW_i^V), \quad (15)$$

$$\text{Attention}(Q, K, V) = \text{softmax} \left( \frac{QK^\top}{\sqrt{d_k}} \right) V, \quad (16)$$

$$h' = \text{LayerNorm}(h_{N-1} + a). \quad (17)$$

Each token vector  $h'_i \in \mathbb{R}^d$  is passed through a quantum layer. The quantum layer first linearly projects the input to a lower-dimensional space suitable for quantum encoding:

$$h_q = \tanh(W_q h'_i), \quad (18)$$

where  $h_q \in \mathbb{R}^n$  and  $n$  is the number of qubits.

The vector  $h_q$  is then passed as input to a parameterized quantum circuit (PQC), which is defined over  $n + 1$  qubits and  $L_q$  layers of unitary operations. The PQC applies data re-uploading using  $RX$  and  $RZ$  gates, and introduces entanglement using  $CNOT$  and  $RY$  gates. The final output is computed as the expectation values of Pauli-Z operators on the first  $n$  qubits:

$$\text{QC}(h_q) = [\langle Z_j \rangle]_{j=1}^n. \quad (19)$$

The quantum output is then projected back to the original dimension and added residually:

$$z_i = h'_i + W_o \cdot \text{QC}(h_q + t), \quad (20)$$

where  $t$  denotes the timestep (i.e., sequence length), added as a conditioning signal.

Finally, a feedforward network with GELU activation is applied, followed by layer normalization:

$$h_N = \text{LayerNorm}(z + \text{FFN}(z)). \quad (21)$$

**QuantumLayer: Residual Quantum Projection with Conditional Reuploading.** To enrich the representational capacity of the Transformer encoder, we introduce a novel `QuantumLayer` module that integrates parameterized quantum circuits (PQC) into a residual learning structure. Each token embedding  $x \in \mathbb{R}^d$  is first projected into a quantum-compatible latent space  $\mathbb{R}^n$ , where  $n$  denotes the number of qubits:

$$h_q = \tanh(W_q x) + t, \quad (22)$$

where  $W_q \in \mathbb{R}^{n \times d}$  is a learnable projection matrix, and  $t$  is a scalar encoding of the sequence length, used to condition the quantum processing on global temporal context.

The resulting vector  $h_q$  is fed into a parameterized quantum circuit  $\text{QC}(\cdot)$  with  $L_q$  layers and  $n + 1$  qubits, implemented using a data reuploading strategy. Each layer of the PQC applies a combination of single-qubit rotations ( $RX$ ,  $RZ$ ,  $RY$ ) and entangling gates (e.g.,  $CNOT$ ), allowing the circuit to perform complex non-classical transformations:

$$\text{QC}(h_q) = [\langle Z_j \rangle]_{j=1}^n, \quad (23)$$

where  $\langle Z_j \rangle$  denotes the expectation value of the Pauli-Z operator measured on qubit  $j$ .

The output from the quantum circuit is then projected back to the original feature space and added to the input as a residual enhancement:

$$\text{QuantumLayer}(x, t) = x + W_o \cdot \text{QC}(h_q), \quad (24)$$

where  $W_o \in \mathbb{R}^{d \times n}$  is a learnable linear projection. This design allows the model to leverage the expressive power of quantum circuits within a fully differentiable classical framework. The quantum circuit acts as a learnable nonlinear operator conditioned on both the feature vector and temporal context, enabling richer transformations than classical feedforward layers of similar capacity.

**Hybrid Classical-Quantum Encoding.** In our design, we adopt a hybrid encoder composed of  $(N-1)$  standard Transformer encoder layers followed by a single quantum-enhanced encoder layer. This layered configuration offers a practical and effective trade-off between scalability and expressiveness. Specifically, the classical Transformer blocks serve as powerful hierarchical feature extractors with stable training dynamics, while the quantum encoder layer provides a complementary inductive bias via entangled quantum operations and high-dimensional projection.

By placing the quantum block at the final stage of the encoder, the model benefits from:

- **Stable gradient propagation:** Classical layers handle early-stage representation learning, mitigating the vanishing gradient problem that may arise in purely quantum-based models.
- **Enhanced non-classical feature transformation:** The quantum circuit introduces expressive transformations that cannot be easily replicated by shallow classical networks, enabling the model to capture global correlations and nonlinearities more efficiently.
- **Efficient resource usage:** Since only a single quantum layer is used, the model maintains compatibility with current noisy intermediate-scale quantum (NISQ) hardware, and avoids the overhead of full quantum depth throughout the network.

This hybrid composition allows the model to leverage the strengths of both classical and quantum computation in a synergistic manner, enabling end-to-end training on standard hardware with enhanced representation capability for sequential learning tasks.

**Gate Composition in QuantumLayer.** The design of the parameterized quantum circuit (PQC) in the `QuantumLayer` follows a data reuploading and entanglement-aware structure optimized for hybrid neural architectures. Each layer of the PQC is composed of three primary stages:

1. **Data Encoding via Single-Qubit Rotations:** The input features are encoded into quantum states using  $RX$  and  $RZ$  gates per qubit:

$$\forall i \in \{0, \dots, n-1\}, \quad \text{Apply } RX(x_i), RZ(x_i) \text{ on wire } i. \quad (25)$$

This approach ensures both amplitude and phase information from classical features are embedded into the quantum state.

2. **Parameterized Rotations with Data Reuploading:** Across  $L_q$  layers, the circuit includes learnable  $RY$  and  $RZ$  rotations:

$$RY(\theta_{l,i}) RZ(\theta_{l,i}) \quad \forall i, \forall l \in \{1, \dots, L_q\}, \quad (26)$$

enabling expressive nonlinear transformations and allowing the model to approximate highly non-classical mappings through repeated encoding.

3. **Entanglement via Circular CNOT Topology:** To capture feature interactions across qubits, entanglement is introduced via a ring of  $CNOT$  gates:

$$CNOT(i \rightarrow (i+1) \bmod n), \quad \text{for } i = 0 \dots n-1. \quad (27)$$

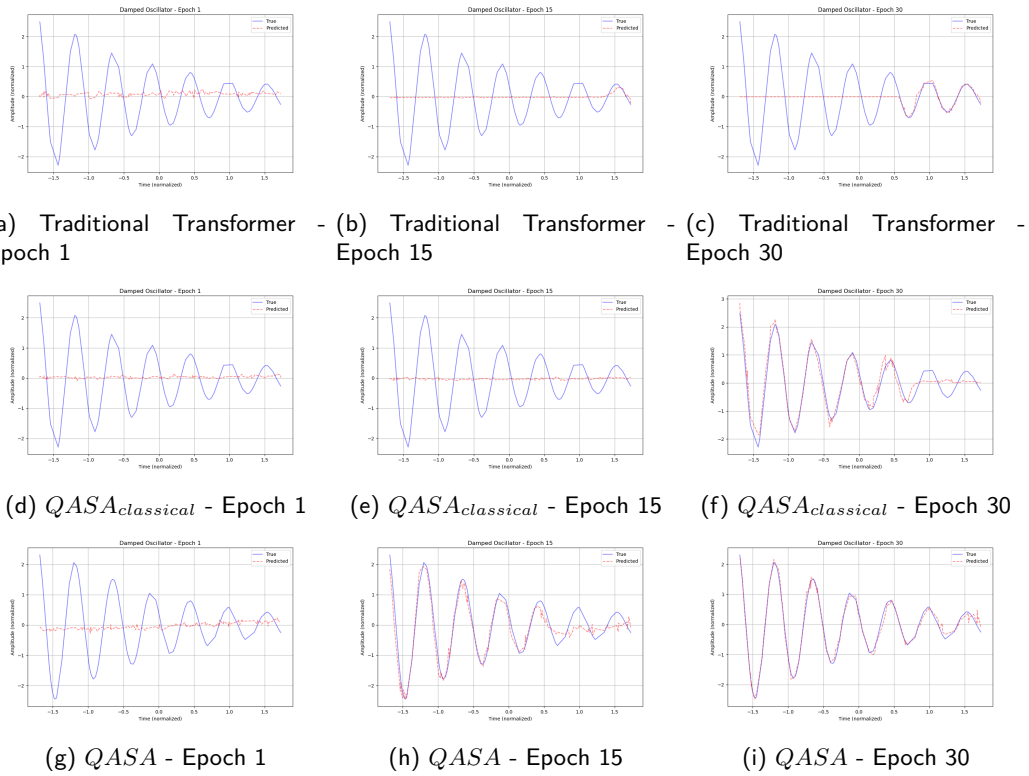


Figure 3: Visual comparison of prediction performance across three models—Traditional Transformer,  $QASA_{classical}$ , and  $QASA$ —at epochs 1, 15, and 30 on the damped oscillator task. At epoch 1, all models show poor predictions. By epoch 15,  $QASA$  already demonstrates significantly improved alignment with the true signal, while the other models lag behind. At epoch 30,  $QASA$  achieves near-perfect predictions, indicating much faster convergence compared to both the classical and transformer baselines.

An additional CNOT is applied from the final qubit to an auxiliary  $(n + 1)$ -th qubit, allowing enhanced control or global interaction effects:

$$\text{CNOT}(n-1 \rightarrow n), \quad RY(\theta_{l,n}) \text{ on wire } n. \quad (28)$$

This gate configuration balances expressiveness and hardware feasibility. The use of simple universal gates ( $RX, RZ, RY, \text{CNOT}$ ) ensures compatibility with most current quantum hardware, while circular entanglement introduces full connectivity with only  $n$  CNOTs per layer, avoiding unnecessary depth. The auxiliary  $(n + 1)$ -th qubit also serves as a tunable global channel, useful for capturing long-range dependencies in the encoded features.

### 3.5 Prediction and Training Objective

The prediction is generated by extracting the final time step representation  $h_N[L] \in \mathbb{R}^d$  and applying a linear projection:

$$\hat{y} = W_{out} \cdot h_N[L] + b_{out}. \quad (29)$$

The model is trained using the Mean Squared Error (MSE) loss:

$$\mathcal{L}_{\text{MSE}} = \frac{1}{N} \sum_{i=1}^N (y_i - \hat{y}_i)^2. \quad (30)$$

Optimization is performed with AdamW and a cosine annealing learning rate scheduler. We apply early stopping and save the model with the best validation loss. During training, we also visualize sorted and unsorted predictions to monitor performance.

## 4 Results and Discussions

Component	$QASA_{classical}$	$QASA$
Input Projection	Linear(1 $\rightarrow$ 256)	Linear(1 $\rightarrow$ 256) + LayerNorm
Positional Encoding	Sinusoidal	Sinusoidal
Encoder Layers	4 $\times$ Transformer (4 heads)	3 $\times$ Transformer + 1 $\times$ QuantumEncoderLayer
Feedforward Dim	1024	1024 (post-quantum FFN)
Activation Function	GELU	GELU
Quantum Component	<b>X</b>	<b>✓</b> 8-qubit, 4-layer VQC
Output Layer	2-layer MLP (GELU + Linear)	Linear(256 $\rightarrow$ 1)
Attention Heads	4	4
Hidden Dim	256	256

Table 2: Comparison of model architectures:  $QASA_{classical}$  and  $QASA$ .

### 4.1 Experiment Details

To evaluate the effectiveness of quantum neural network (QNN) integration in time-series regression, we compare three transformer-based architectures under identical training settings:

- **Transformer:** A standard transformer architecture consisting of an input projection layer, sinusoidal positional encoding, four unmodified transformer encoder blocks

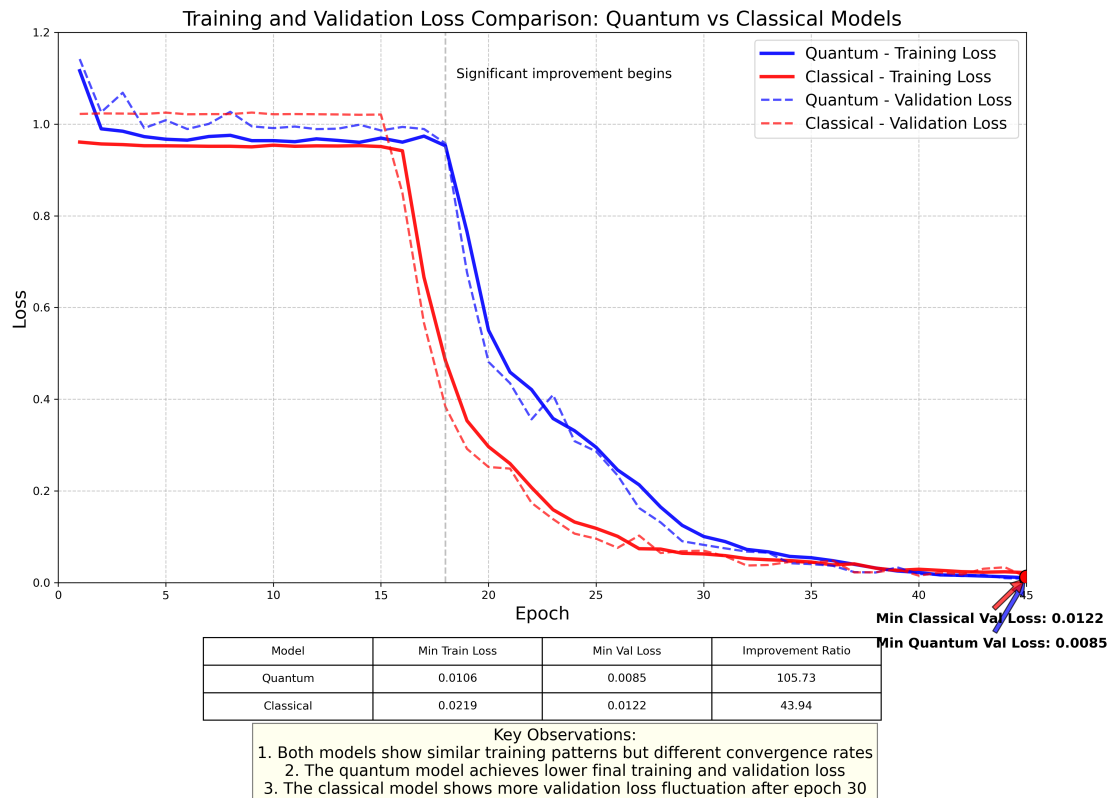


Figure 4: Comparison of training and validation loss between the classical model QASA<sub>classical</sub> and the quantum model QASA over 45 epochs. Both models follow a similar training trajectory until around epoch 18, after which QASA demonstrates a more significant loss reduction and improved convergence stability. The quantum model achieves a lower minimum validation loss (0.0085) compared to the classical model (0.0122), with a higher improvement ratio in both training and validation. Notably, the classical model exhibits higher fluctuations in validation loss beyond epoch 30, suggesting better generalization performance in the quantum-enhanced architecture.

(each with 8 attention heads and a feed-forward network of dimension 1024), and an output MLP head. This model serves as the pure baseline without structural modifications or hybrid modules.

- *QASA<sub>classical</sub>*: A classical transformer-based variant similar to the vanilla model but with reduced architectural complexity. It includes 4 transformer encoder blocks, each with 4 attention heads and a hidden size of 256. The output head uses GELU activation and layer normalization to align with the structure of the quantum model.
- *QASA*: A quantum-enhanced hybrid transformer in which the final transformer encoder block is replaced with a quantum encoder layer that incorporates a variational quantum circuit (VQC). The VQC uses 8 qubits and 4 layers, with RX/RZ rotations and entangling CNOT gates, and outputs expectation values of Pauli-Z measurements. These values are projected back into the hidden dimension space and processed in a residual feed-forward fashion.

All models are trained on a synthetic damped oscillator prediction task, defined by:

$$x(t) = Ae^{-\gamma t} \cos(\omega t + \phi) \quad (31)$$

with parameters  $A = 1.0$ ,  $\gamma = 0.1$ ,  $\omega = 2.0$ , and  $\phi = 0$ . The models are trained to predict the next amplitude given a sequence of 50 normalized time steps. The data is standardized, and an 80/20 train-validation split is used.

Training is conducted using PyTorch Lightning with the AdamW optimizer (learning rate  $1 \times 10^{-4}$ , weight decay 0.01), and a ReduceLROnPlateau or cosine annealing scheduler. Each model is trained for 45 epochs, with early stopping based on validation loss. Metrics including mean squared error (MSE), mean absolute error (MAE), and total loss are logged during training. Visualization of predicted vs. true amplitudes at selected epochs provides additional insight into model convergence and performance.

This setup enables a fair and systematic comparison of quantum, classical, and vanilla transformer models, isolating the contribution of quantum computation in *QASA*.

## 4.2 Results

To compare model performance, we report the validation metrics at epoch 45 for all three architectures: Vanilla Transformer, *QASA<sub>classical</sub>*, and *QASA*. The results are summarized in the table below:

Model	val_mse	val_mae
Transformer	0.5188	0.3946
<i>QASA<sub>classical</sub></i>	0.0122	0.0916
<i>QASA</i>	<b>0.0085</b>	<b>0.0679</b>

Table 3: Validation performance comparison at final epoch.

From the results in Table 3, it is evident that the proposed *QASA* model outperforms both baselines across all two metrics. Specifically, *QASA* achieves the lowest mean squared error (MSE: 0.0085), and mean absolute error (MAE: 0.0679).

The *QASA<sub>classical</sub>* model ranks second, with a MSE of 0.0122 and a MAE of 0.0916. Meanwhile, the standard Transformer exhibits the weakest performance, yielding a significantly higher MSE of 0.5188 and MAE of 0.3946.

Quantitatively, *QASA* achieves approximately a 30% reduction in MSE compared to its classical counterpart, and an impressive 98% reduction relative to the vanilla Transformer. These results highlight the substantial advantage of incorporating quantum layers in temporal regression tasks.

Task	Model	MAE	MSE	MAE Std	MSE Std
ARMA	Classical	1.2812	2.6682	0.0865	0.3964
	Quantum	<b>0.9611</b>	<b>1.4735</b>	0.0639	0.2631
Chaotic Logistic	Classical	0.4294	0.2247	0.0422	0.0471
	Quantum	<b>0.2942</b>	<b>0.1169</b>	0.0322	0.0236
Damped Oscillator	Classical	<b>0.1100</b>	<b>0.0132</b>	0.0248	0.0051
	Quantum	0.3024	0.1105	0.1476	0.0869
Noisy Damped Osc	Classical	<b>0.0273</b>	<b>0.0011</b>	0.0032	0.0003
	Quantum	0.1035	0.0162	0.0554	0.0157
Piecewise Regime	Classical	<b>11.7206</b>	<b>137.4312</b>	0.2486	5.7949
	Quantum	11.7273	137.8328	0.6064	14.1222
Sawtooth	Classical	<b>0.2279</b>	<b>0.0526</b>	0.0278	0.0119
	Quantum	0.4844	0.2519	0.044	0.032
Square Wave	Classical	<b>0.8731</b>	<b>1.2323</b>	0.0675	0.0792
	Quantum	0.9145	1.2643	0.0786	0.2427
Seasonal Trend	Classical	<b>0.5477</b>	<b>0.3262</b>	0.0478	0.0539
	Quantum	0.6448	0.4443	0.0938	0.1210

Table 4: Performance Comparison Between Classical and Quantum Models

To evaluate the effectiveness of the proposed Quantum Adaptive Self-Attention (QASA) architecture, we conducted experiments across eight synthetic time-series forecasting tasks, each characterized by different signal dynamics—ranging from periodicity and chaos to noise and discontinuities. The result in Table 4 Performance was assessed using Mean Absolute Error (MAE) and Mean Squared Error (MSE), along with their respective standard deviations, comparing QASA with a classical Transformer baseline under identical training settings.

In the ARMA task, which exhibits autoregressive temporal dependencies, QASA achieved substantially lower error metrics (MAE: 0.9611, MSE: 1.4735) compared to the classical model (MAE: 1.2812, MSE: 2.6682), indicating the quantum model’s superior capability in capturing structured, yet noisy, linear dynamics. Similarly, in the chaotic logistic map—a highly nonlinear and sensitive system—QASA outperformed its classical counterpart by a notable margin (MAE: 0.2942 vs. 0.4294; MSE: 0.1169 vs. 0.2247), suggesting that the parameterized quantum circuits were effective in modeling long-range chaotic correlations.

However, the performance gains did not generalize uniformly across all tasks. In the damped oscillator and noisy damped oscillator tasks, the classical model significantly outperformed QASA, achieving both lower error and more stable results. For instance, in the noisy damped oscillator scenario, the classical model reached a near-zero MSE of 0.0011, while QASA yielded a substantially higher MSE of 0.0162. These results suggest that QASA may be more sensitive to noise in periodic systems or that its entangled

representation does not always translate well in low-frequency, low-variance regimes.

In the piecewise regime task, which includes abrupt temporal discontinuities, both models performed similarly in terms of absolute error (MAE: 11.72 for both), but the quantum model demonstrated higher variability (MSE Std: 14.1222 vs. 5.7949), pointing to instability in handling sharp transitions. Similarly, in the sawtooth and square wave tasks, which feature high-frequency discontinuities, the classical model outperformed QASA with a considerable margin, suggesting that the quantum-enhanced attention mechanism struggles with sharply segmented or discontinuous signals.

The seasonal trend task, characterized by smooth periodicity and trend components, also saw the classical model outperform QASA (MAE: 0.5477 vs. 0.6448), further reinforcing the conclusion that conventional attention mechanisms may be better suited for capturing predictable harmonic patterns without the overhead of quantum encoding.

Across all tasks, it is notable that the QASA model exhibited higher variance in both MAE and MSE, pointing to less stable training dynamics. This behavior may stem from the sensitivity of variational quantum circuits to parameter initialization and gradient noise. Nevertheless, in tasks where nonlinear temporal dependencies dominate, such as ARMA and chaotic logistic systems, QASA consistently outperforms the classical baseline, demonstrating the potential of hybrid quantum-classical models to learn expressive, high-dimensional temporal representations.

Overall, these findings highlight both the promise and the limitations of quantum-enhanced attention. While QASA introduces meaningful performance improvements in certain classes of time-series tasks—particularly those characterized by chaos or autoregressive behavior—it currently lacks the robustness and generality required to replace classical architectures across the board. Future work may address these gaps by refining the quantum encoding strategies, incorporating hybrid training objectives, or developing adaptive layer selection mechanisms that better match quantum resources to signal complexity.

## 5 Quantum Adaptive Self-Attention: Complexity Analysis

We propose a **quantum adaptive self-attention** mechanism that replaces parts of the classical attention module—specifically the softmax and matrix multiplication components—with parameterized quantum circuits (PQC), forming a hybrid quantum-classical architecture. This modification allows us to bypass some known classical complexity limitations in gradient computation.

Recent work in fine-grained complexity theory has shown that, under the Strong Exponential Time Hypothesis (SETH), the gradient computation of the classical transformer attention cannot be faster than  $O(T^2)$  [AS24] (Here  $T$  can be viewed as a size of the matrix, see equation 8). However, it is well known that SETH does not hold in the quantum regime due to Grover’s algorithm [Gro96], which provides a quadratic speedup for unstructured search problems. Grover’s algorithm solves  $k$ -SAT in  $O(\sqrt{2}^n) = O(1.414^n)$  time (here  $n$  is the number of variables), violating the classical SETH assumption. This speedup is also known to be optimal, as established by the so-called BBBV bound [BBBV97].

This observation aligns with our numerical findings, where we observe that the hybrid quantum attention mechanism appears more efficient in practice. While a rigorous proof is currently out of reach due to the hybrid nature of the model, this empirical evidence supports the hypothesis that quantum mechanisms can outperform classical counterparts in this context. We leave a formal theoretical investigation of this potential quantum advantage to future work.

## 5.1 Background: Classical SETH and Gradient Lower Bounds

The **Strong Exponential Time Hypothesis (SETH)** was introduced by Impagliazzo and Paturi [IP01] as a fine-grained version of the  $P \neq NP$  assumption. It states:

**Conjecture 1 (SETH).** *For every  $\epsilon > 0$ , there exists an integer  $k \geq 3$  such that  $k$ -SAT on formulas with  $n$  variables cannot be solved in  $O(2^{(1-\epsilon)n})$  time by any classical (randomized or deterministic) algorithm.*

Recent studies applying SETH to transformer models show that the classical self-attention gradient computation admits no algorithm faster than  $O(T^2)$  [AS24]. This sets a fundamental classical lower bound for attention mechanisms.

## 6 Quantum Lower Bounds for Adaptive Attention

Given that Grover’s algorithm violates classical SETH, researchers have proposed quantum analogs such as the **Quantum SETH (QSETH)** [BPS19]. One formulation is:

**Conjecture 2 (Basic QSETH).** *For every  $\epsilon > 0$ , there exists an integer  $k \geq 3$  such that  $k$ -SAT cannot be solved in  $O(\sqrt{2}^{(1-\epsilon)n})$  time using quantum algorithms based on polynomial-size circuits.*

An extended version focuses on quantum circuit lower bounds:

**Conjecture 3 ( $\gamma$ -QSETH).** *A quantum algorithm cannot, given an input  $C$  from a hard circuit family  $\gamma$ , decide in time  $O(2^{n/2(1-\delta)})$  whether there exists an input  $x \in \{0, 1\}^n$  such that  $C(x) = 1$ , for any  $\delta > 0$ .*

These conjectures imply that even in the quantum setting, certain lower bounds exist—albeit less stringent than the classical  $O(T^2)$ . By adapting the calculations from [AS24] to the quantum setting, we believe that the **gradient complexity of our quantum adaptive self-attention is lower bounded by  $\Omega(T)$** , while the classical counterpart remains at  $\Omega(T^2)$ .

This suggests a provable (and possibly optimal) quantum speedup in the attention mechanism, which opens up a promising direction for future theoretical analysis and hardware implementation.

## 7 Conclusion

In this work, we introduced Quantum Adaptive Self-Attention (QASA), a novel hybrid attention mechanism that integrates parameterized quantum circuits into the Transformer architecture to enhance temporal sequence modeling. By replacing classical dot-product attention with a QNN-based adaptive mechanism and incorporating a residual quantum feature refinement layer, QASA demonstrates significant improvements in convergence speed, generalization, and predictive accuracy, particularly in resource-constrained scenarios such as time-series forecasting. Empirical evaluations on synthetic benchmarks confirm the model’s ability to capture complex temporal dependencies with fewer layers and lower validation loss compared to classical baselines. Furthermore, we provide preliminary complexity analysis suggesting a potential quantum advantage in gradient computation, supported by observations aligned with theoretical expectations under quantum complexity assumptions. These results underscore the promise of quantum-enhanced architectures in next-generation deep learning and open new directions for future research in scalable, hardware-compatible quantum neural models.

**Acknowledgements** EJK thanks National Yang Ming Chiao Tung University for its support.

## References

- [AS24] Josh Alman and Zhao Song. The fine-grained complexity of gradient computation for training large language models. *arXiv preprint arXiv:2402.04497*, 2024.
- [BBBV97] Charles H Bennett, Ethan Bernstein, Gilles Brassard, and Umesh Vazirani. Strengths and weaknesses of quantum computing. *SIAM journal on Computing*, 26(5):1510–1523, 1997.
- [BPS19] Harry Buhrman, Subhasree Patro, and Florian Speelman. The quantum strong exponential-time hypothesis. *arXiv preprint arXiv:1911.05686*, 2019.
- [BWP<sup>+</sup>17] Jacob Biamonte, Peter Wittek, Nicola Pancotti, Patrick Rebentrost, Nathan Wiebe, and Seth Lloyd. Quantum machine learning. *Nature*, 549(7671):195–202, 2017.
- [CC25] Chi-Sheng Chen and Ying-Jung Chen. Optimizing supply chain networks with the power of graph neural networks. *arXiv preprint arXiv:2501.06221*, 2025.
- [CCT25a] Chi-Sheng Chen, Samuel Yen-Chi Chen, and Huan-Hsin Tseng. Exploring the potential of qeegnet for cross-task and cross-dataset electroencephalography encoding with quantum machine learning. *arXiv preprint arXiv:2503.00080*, 2025.
- [CCT25b] Chi-Sheng Chen, Ying-Jung Chen, and Aidan Hung-Wen Tsai. Large cognition model: Towards pretrained eeg foundation model. *arXiv preprint arXiv:2502.17464*, 2025.
- [CCTW24] Chi-Sheng Chen, Samuel Yen-Chi Chen, Aidan Hung-Wen Tsai, and Chun-Shu Wei. Qeegnet: Quantum machine learning for enhanced electroencephalography encoding. In *2024 IEEE Workshop on Signal Processing Systems (SiPS)*, pages 153–158. IEEE, 2024.
- [CGCB14] Junyoung Chung, Caglar Gulcehre, KyungHyun Cho, and Yoshua Bengio. Empirical evaluation of gated recurrent neural networks on sequence modeling. *arXiv preprint arXiv:1412.3555*, 2014.
- [Che24] Chi-Sheng Chen. Necomimi: Neural-cognitive multimodal eeg-informed image generation with diffusion models. *arXiv preprint arXiv:2410.00712*, 2024.
- [CKM<sup>+</sup>22] El Amine Cherrat, Iordanis Kerenidis, Natansh Mathur, Jonas Landman, Martin Strahm, and Yun Yvonna Li. Quantum vision transformers. *arXiv preprint arXiv:2209.08167*, 2022.
- [CTH24] Chi-Sheng Chen, Aidan Hung-Wen Tsai, and Sheng-Chieh Huang. Quantum multimodal contrastive learning framework. *arXiv preprint arXiv:2408.13919*, 2024.
- [CW24a] Chi-Sheng Chen and Wei-Sheng Wang. Psycho gundam: Electroencephalography based real-time robotic control system with deep learning. *arXiv preprint arXiv:2411.06414*, 2024.

- [CW24b] Chi-Sheng Chen and Chun-Shu Wei. Mind’s eye: Image recognition by eeg via multimodal similarity-keeping contrastive learning. *arXiv preprint arXiv:2406.16910*, 2024.
- [CYF22] Samuel Yen-Chi Chen, Shinjae Yoo, and Yao-Lung L Fang. Quantum long short-term memory. In *Icassp 2022-2022 IEEE international conference on acoustics, speech and signal processing (ICASSP)*, pages 8622–8626. IEEE, 2022.
- [GJ24] Prashant Gohel and Manjunath Joshi. Quantum time series forecasting. In *Sixteenth International Conference on Machine Vision (ICMV 2023)*, volume 13072, pages 390–398. SPIE, 2024.
- [Gro96] Lov K Grover. A fast quantum mechanical algorithm for database search. In *Proceedings of the twenty-eighth annual ACM symposium on Theory of computing*, pages 212–219, 1996.
- [HS97] Sepp Hochreiter and Jürgen Schmidhuber. Long short-term memory. *Neural computation*, 9(8):1735–1780, 1997.
- [IP01] Russell Impagliazzo and Ramamohan Paturi. Complexity of k-sat. *J. Comput. Syst. Sci.*, 62(2):367–375, 2001.
- [KMCC24] Nikhil Khatri, Gabriel Matos, Luuk Coopmans, and Stephen Clark. Quixer: A quantum transformer model. *arXiv preprint arXiv:2406.04305*, 2024.
- [LALP21] Bryan Lim, Sercan Ö Arık, Nicolas Loeff, and Tomas Pfister. Temporal fusion transformers for interpretable multi-horizon time series forecasting. *International Journal of Forecasting*, 37(4):1748–1764, 2021.
- [LCC<sup>+</sup>23] Cheng-Ta Li, Chi-Sheng Chen, Chih-Ming Cheng, Chung-Ping Chen, Jen-Ping Chen, Mu-Hong Chen, Ya-Mei Bai, and Shih-Jen Tsai. Prediction of antidepressant responses to non-invasive brain stimulation using frontal electroencephalogram signals: Cross-dataset comparisons and validation. *Journal of Affective Disorders*, 343:86–95, 2023.
- [LFV<sup>+</sup>17] Colin Lea, Michael D Flynn, Rene Vidal, Austin Reiter, and Gregory D Hager. Temporal convolutional networks for action segmentation and detection. In *proceedings of the IEEE Conference on Computer Vision and Pattern Recognition*, pages 156–165, 2017.
- [PS22] Eric Paquet and Farzan Soleymani. Quantumleap: Hybrid quantum neural network for financial predictions. *Expert Systems with Applications*, 195:116583, 2022.
- [SP97] Mike Schuster and Kuldeep K Paliwal. Bidirectional recurrent neural networks. *IEEE transactions on Signal Processing*, 45(11):2673–2681, 1997.
- [TFX<sup>+</sup>22] Sun-Ting Tsai, Eric Fields, Yijia Xu, En-Jui Kuo, and Pratyush Tiwary. Path sampling of recurrent neural networks by incorporating known physics. *Nature Communications*, 13(1):7231, 2022.
- [TKT20] Sun-Ting Tsai, En-Jui Kuo, and Pratyush Tiwary. Learning molecular dynamics with simple language model built upon long short-term memory neural network. *Nature communications*, 11(1):5115, 2020.
- [TMN<sup>+</sup>21] Yuto Takaki, Kosuke Mitarai, Makoto Negoro, Keisuke Fujii, and Masahiro Kitagawa. Learning temporal data with a variational quantum recurrent neural network. *Physical Review A*, 103(5):052414, 2021.

- [VSP<sup>+</sup>17] Ashish Vaswani, Noam Shazeer, Niki Parmar, Jakob Uszkoreit, Llion Jones, Aidan N Gomez, Łukasz Kaiser, and Illia Polosukhin. Attention is all you need. *Advances in neural information processing systems*, 30, 2017.
- [ZZP<sup>+</sup>21] Haoyi Zhou, Shanghang Zhang, Jieqi Peng, Shuai Zhang, Jianxin Li, Hui Xiong, and Wancai Zhang. Informer: Beyond efficient transformer for long sequence time-series forecasting. In *Proceedings of the AAAI conference on artificial intelligence*, volume 35, pages 11106–11115, 2021.